JOURNAL OF GEOPHYSICAL RESEARCH, VOL. 100, NO. D7, PAGES 14,089–14,096, JULY 20, 1995

Space-time integrity of improved stratospheric and mesospheric sounder and microwave limb sounder temperature fields at Kelvin wave scales

E. M. Stone, J. L. Stanford, J. R. Ziemke, and D. R. Allen

Department of Physics and Astronomy, Iowa State University, Ames

F. W. Taylor, C. D. Rodgers, and B. N. Lawrence

Department of Atmospheric, Oceanic, and Planetary Physics, University of Oxford, Oxford, England

E. F. Fishbein, L. S. Elson, and J. W. Waters

Jet Propulsion Laboratory, California Institute of Technology, Pasadena

Abstract. Space-time analyses, which are sensitive to details of retrieval and gridding processes not seen in zonal and time means, are used to investigate the integrity of version 8 gridded retrieved temperatures from the improved stratospheric and mesospheric sounder (ISAMS) on the upper atmosphere research satellite (UARS). This note presents results of such analyses applied to ISAMS tropical data. Comparisons are made with microwave limb sounder (MLS), also on UARS, temperatures. Prominent zonal wave number 1 features are observed with characteristics similar to those expected for Kelvin waves. Time versus longitude plots reveal quasi-regular eastward phase progression from November 1991 to mid-January 1992. The perturbations extend throughout the upper stratosphere and lower mesosphere (altitudes of 32–64 km), exhibiting peak-to-peak amplitudes of up to 2°–3° K and periods from ~ 2 weeks in midstratosphere to ~ 1 week at higher altitudes. Faster Kelvin waves with periods of 3–5 days are also found in the lower mesosphere. Height versus time plots reveal downward phase and upward group velocities, consistent with forcing from below. Vertical wavelengths are ~ 20 km for the slower mode and about twice this scale for the faster 3 to 5-day mode. The features are trapped within ±10°–15° of the equator. Kelvin wave signatures in ISAMS and MLS temperatures are compared at 10 and 1 hPa. Good agreement is found, illustrating the internal consistency and ability of both ISAMS and MLS temperature grids to capture relatively small amplitude features with space-time scales of fast, zonally asymmetric equatorial modes.

1. Introduction

The primary objective of this paper is to demonstrate the space-time integrity of improved stratospheric and mesospheric sounder (ISAMS) and microwave limb sounder (MLS) temperature grids through investigation of equatorial Kelvin wave signatures. Because space-time spectral analysis provides a rather sensitive tool for investigating details which may be obscured in zonal means and time averages, these results provide a measure of validation of retrieval and gridding processes.

Evidence for equatorial Kelvin modes in the upper stratosphere and lower mesosphere have been reported by *Hirota* [1978] using rocketsonde data and by *Salby et al.* [1984] using limb infrared monitor of the stratosphere (LIMS) (on Nimbus 7) temperature data. Kelvin waves have been reported in middle atmosphere constituents by *Randel* [1990] in LIMS ozone, water vapor, nitric acid and nitrogen dioxide data, by *Salby et al.* [1990] in LIMS ozone and nitrogen dioxide data, by *Prata* [1990] and *Hirota et al.* [1991] in solar backscattered ultraviolet (SBUV) ozone data, by *Randel and Gille* [1991] in SBUV and LIMS ozone data, and by *Ziemke and Stanford* [1994] in total ozone measurements from the total ozone mapping spectrometer instrument. Kelvin waves are important because of their dynamical forcing of middle atmosphere circulation. For example, there is evidence that they provide a major component of the forcing required to accelerate the eastward wind phase of the quasi-biennial oscillation [*Andrews et al.*, 1987]. Kelvin waves are also involved in the eastward forcing of the semiannual oscillation, but it is yet uncertain whether they are the primary forcing agent.

Paper number 95JD01171.
0148-0227/95/95JD-01171$05.00

We next briefly describe the ISAMS and MLS instruments, data, and the analysis procedures used here. We then present evidence that ISAMS equatorial temperature fields contain Kelvin-wave-like signals throughout much of the upper stratosphere and lower mesosphere. The clarity of the waves is indicative of ISAMS's ability to capture relatively small amplitude temperature perturbations on these spatial and temporal scales. Finally, comparison is made between Kelvin wave signatures in ISAMS and MLS data. The agreement is shown to be good, enhancing confidence in both data sets.

2. The ISAMS and MLS Instruments and Data

ISAMS Instrument

ISAMS, one of 10 upper atmosphere research satellite (UARS) instruments, is an infrared gas correlation radiometer with absolute radiometric calibration, using both wideband techniques and pressure-modulated cells containing a number of the trace gases to be observed. The instrument is a limb sounder, observing thermally emitted atmospheric radiation at the limb of the Earth. ISAMS, alone amongst the UARS stratospheric sounders, had the capacity to view both sides of the spacecraft. The general pressure modulation technique [*Taylor*, 1983] has been successfully used for years on meteorological satellites, including the predecessor instrument, the stratospheric and mesospheric sounder on Nimbus 7 and the stratospheric sounder unit (SSU) instruments which have played a vital role in obtaining the observational database for the stratosphere. ISAMS is described in the UARS Project Data Book (NASA Goddard Space Flight Center, General Electric, Astro-Space Division, Greenbelt, Maryland, 1987) and by *Taylor et al.* [1993].

MLS Instrument

The microwave limb sounder, another UARS instrument, uses a 1.6-m scanning antenna to observe the limb of the atmosphere simultaneously in spectral bands at 63, 183, and 205 GHz [*Barath et al.*, 1993]. These observations allow the determination of chlorine monoxide, ozone, water vapor, and temperature in the stratosphere and mesosphere during both day and night and in the presence of stratospheric clouds and aerosols. Details of temperature retrieval techniques, accuracies and validation have been described by *Fishbein et al.* [1995].

Data

In spite of early failure of the ISAMS instrument, global data records of approximately 6 months total have been obtained from ISAMS. This study uses 83 continuous days, October 28, 1991–January 18, 1992, of ISAMS version 8 along-track (L3AT) temperature data which have been globally gridded. The data were synoptically gridded for 12GMT, using an objective analysis scheme which weighted all data within 2000 km and 12 hours of the output grid points. The weighting factors were chosen so that the e-folding influence in distance and time were 500 km and 6 hours. The gridding scheme was validated by gridding along-track stratospheric sounding unit (SSU) data and comparing the resulting analysis with the United Kingdom Meteorological Office (UKMO) analysis. The output grid chosen retained the full vertical resolution of the data, resulting in 36 levels, from 237 hPa to 0.01 hPa (1.43 to 11.51 scale heights, respectively, one scale height chosen to be 6950 m). Note, however, that ISAMS did not measure below 100 hPa altitude and the version 8 retrievals are largely climatology above 0.1 hPa [*Rodgers et al.*, 1994]. Details about the ISAMS temperature retrievals are given by *Dudhia and Livesey* [1995]. The horizontal grid has spacings of 10° in longitude and 5° in latitude, beginning at 0°E and 87.5°S, respectively.

The MLS data described here were produced as described in *Elson and Froidevaux* [1993]. This process, based on work by *Salby* [1982a, b] and *Lait and Stanford* [1988], involves rotating the space and time coordinates to a suitable system where fast Fourier transforms (FFTs) can be used to calculate the space-time spectral coefficients. The procedure uses time ordered (level 3AT) data but is generally limited to short (~1 week) analysis periods by drift in the UARS orbital period. Inverse transforms convert the coefficients to synoptic maps (i.e., one output time for all latitude/longitude grid points). The synoptic maps are gridded with 5 degree longitude by 4 degree latitude spacings. These maps were then analyzed by the approach described next in section 3.

3. Analysis Procedure

Space-time spectra were computed using an 84-day window length. Data from day 83 (January 18,1992) were copied to form day 84 to provide an even-numbered series length for convenience in spectral analyses. During the calculation of power spectra, time series averages were removed and a 10%–10% cosine taper window applied to reduce leakage. These power spectra calculations also included a decomposition in space-time variables into eastward and westward components [see the appendix of *Ziemke and Stanford*, 1990], no effort was made to remove standing wave variability in the data. A 0.25–0.5–0.25 running mean was applied once to the raw power ordinates as a spectral estimator. Raw power spectra ordinates are defined in this study by $(2\Delta f)^{-1}[A^2(k,\omega) + B^2(k,\omega)]$, where Δf is the unit bandwidth (1 d^{-1} here). $A(k,\omega)$ and $B(k,\omega)$ are calculated via fast Fourier transform (FFT) in both time

and space from the following zonal space-time harmonic definition for temperature T:

$$T_{\pm}(x,t) = \sum_{k=0}^{\pi/\Delta x} \sum_{\omega=0}^{\pi/\Delta t} \Big[A_{\pm}(k,\omega)\cos(kx \pm \omega t) + B_{\pm}(k,\omega)\sin(kx \pm \omega t) \Big]. \quad (1)$$

Here t (x) denotes time (zonal distance), Δt is the temporal sampling interval equal to 1 day, Δx is the spatial sampling interval of $\frac{2\pi a \cdot \cos\phi}{36}$, k is the zonal wave number with units of per meter, ω is the circular frequency, a is the Earth's radius, ϕ is latitude and + (−) denotes the westward (eastward) propagating component of T. The band-pass filter response function given by *Murakami* [1979] was applied in frequency space (using an inverse FFT) to reconstruct band-pass filtered time series.

4. Results

Characteristics of Kelvin Waves

The rocket and satellite data analyses noted in the introduction have revealed Kelvin waves in the upper stratosphere and lower mesosphere with periods in the range of 5–10 days and vertical wavelengths of 10–40 km. The fast Kelvin wave is observed to have periods of 3 to 5 days and vertical wavelengths of 40 km. The waves have eastward phase movement and occur episodically. Their downward phase propagation is consistent with upward energy flux, presumably being excited in the troposphere below. These observations are consistent with theoretical predictions based on the linearized primitive equations of motion on an equatorial beta plane [*Andrews et al.*, 1987]. The theory predicts low latitude confinement for the disturbances, which is also observed. We next examine analyses of ISAMS temperature fields and show that they contain wavelike perturbations similar to those described above for Kelvin waves.

ISAMS Analyses

Figure 1 shows the power spectrum for zonal wave number 1 (one wavelength fits around the equator) ISAMS temperature fields at the equator. Wave number 2 showed less clear Kelvin wave signatures in unfiltered ISAMS data and is not discussed here. In Figures 1–3, 5, and 6 "equator" is defined to be the average of data at the 2.5°N and 2.5°S latitude grid points. Altitude is plotted on the vertical axis, and the periods of eastward and westward moving wave 1 perturbations are indicated on the right and left horizontal axes. The westward features are presumably Rossby modes. In this paper we focus on the eastward spectral features.

The eastward moving perturbations exhibit enhanced spectral power in a band of periods extending from near 12 days at 10 hPa (32 km altitude) to about a week at 1 hPa (48 km altitude) in Figure 1. A second band of enhanced power is seen from 0.75 hPa to 0.1 hPa with a period of 3 to 4 days. In ISAMS version 8 the retrievals were increasingly relaxed to climatology at altitudes above 0.1 hPa.

On the basis of these spectral band results, the data were band-pass filtered with half amplitude response at 4- and 16-day periods to study the first band of spec-

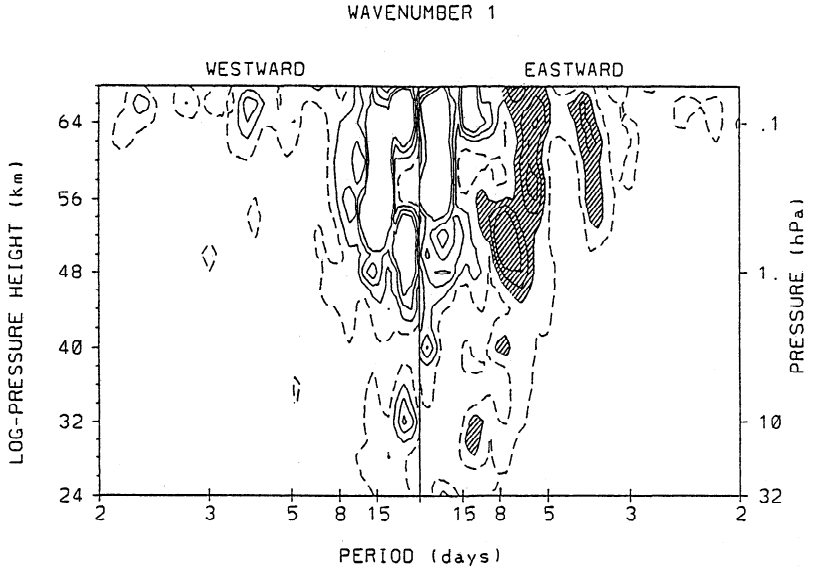

Figure 1. Log-pressure height versus frequency (periods in days shown) westward/eastward equatorial zonal wave 1 ISAMS temperature power spectra (see section 3). Dashed contours are 0.02 K^2-day. Solid contours start at 0.04 and increment by 0.02 K^2-day up to 0.08 K^2-day. Shaded regions denote the Kelvin wave discussed in section 4.

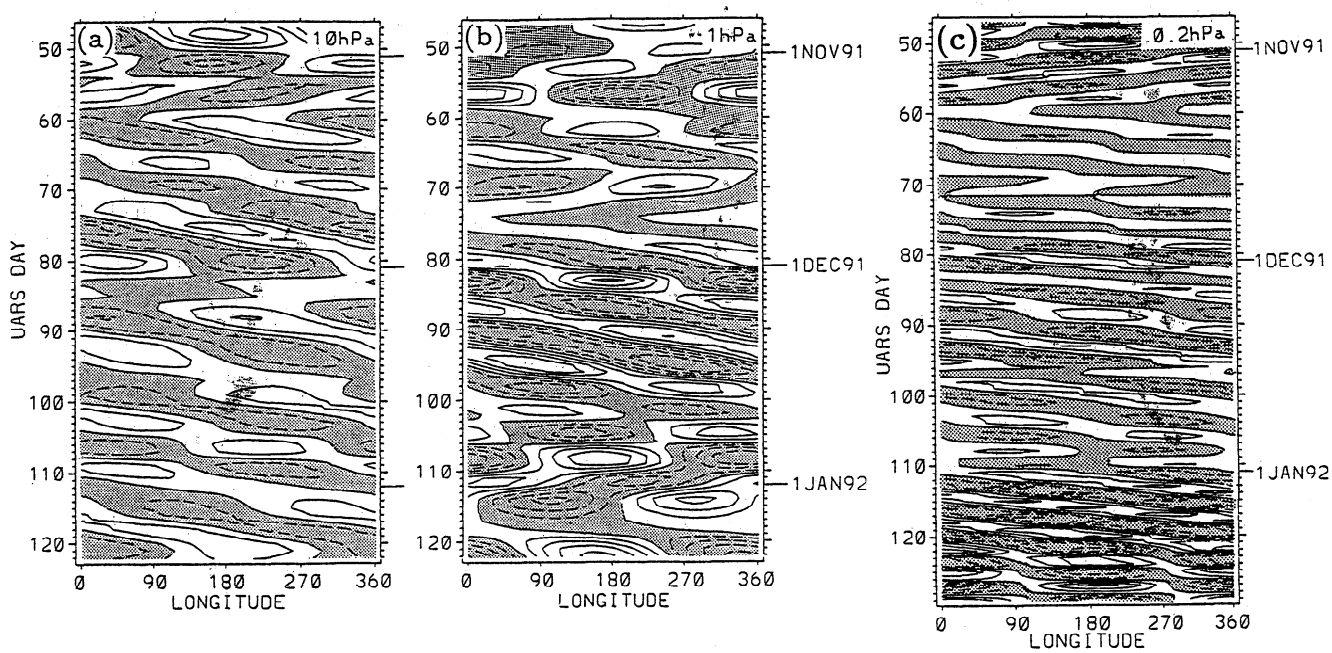

Figure 2. Time versus longitude Hovmöller diagrams of equatorial zonal wave 1 ISAMS band-passed temperatures for (a) 10 hPa, (b) 1 hPa, and (c) 0.2 hPa heights (altitudes of ~32, ~48, and ~59 km, respectively). Band-pass filtering: half-amplitude filter response at 4- and 16-day periods in Figures 2a and 2b, 3- to 5-day periods in Figure 2c. Solid (dashed) contours begin at zero (-0.5) and increment (decrement) by 0.5. Units are Kelvin. Regions with negative perturbation temperatures are shaded.

tral power and with half amplitude response at 3 and 5 days to analyze the second band. Reconstructed wave 1 band-passed temperature fields at 10, 1, and 0.2 hPa are shown in Figure 2. Peak-to-peak temperature perturbations are 2–3 K. The contours of temperature reveal clear episodes of eastward phase progression in which the longitude of constant phase lines moves eastward with time. This is especially clear during UARS days 86 (early December 1991) to 121 (beginning of January 1992) at 10 hPa, 76 to 101 at 1 hPa and 77 to the end of the record at 0.2 hPa. The latter 20 days or so of the record contain particularly strong signals at the highest altitude, 0.2 hPa (58 km), in the lower mesosphere.

The vertical structure of the features and their time variation may be further examined with the aid of Figure 3. A pronounced packet of waves at 1 hPa and above is observed (Figure 3a) for about a month, starting around UARS day 76 (near the end of November 1991). Downward phase progression with time is evident. Upward group velocity (packet envelope movement) can also be discerned in the lower levels. Both phase and group velocity are consistent with forcing from below. The average period of oscillations in this wave packet is about 6 days in the upper levels. Near 10 hPa the periods are somewhat longer. Identifiable downward phase motions can also be seen early in the record, during days 47–76 at 10 to 1 hPa, and again in the latter part of the record. Such episodic behavior is reminiscent of Kelvin wave behavior observed in LIMS data [*Salby et al.*, 1984].

The features exhibit longer periods, ~ 2 weeks, in midstratosphere, decreasing to ~ 6 days at 0.1–1 hPa. In addition to this slower Kelvin mode, a faster feature is found in the lower mesosphere, with 3 to 5-day periods.

In Figure 3b the vertical structure of the faster mode is seen. Near the end of December 1991 a relatively intense wave packet with downward phase progression occurs at upper levels (0.1–1 hPa). The phase tilt of this mode is more uniform in height than that seen in Figure 3a. These results are similar to a wave number 1 Kelvin wave feature with a period of 3.5–4.0 days seen in LIMS temperature data [*Salby et al.*, 1984].

Largest temperature amplitudes appearing at the highest levels in Figure 3a and 3b indicate the presence of a strong shear of the zonal wind with height. Tropical zonal winds are described as large and negative in the higher levels shown in Figure 3, due to the westward wind phase of the semiannual oscillation at these heights around December and January [see *Andrews et al.* 1987]. The data assimilation model winds (from the UKMO) shown by *Canziani et al.* [1994] in their Figure 1a confirm these anticipated large westward winds around the stratopause during these months. Returning to Figure 3, amplitudes for both the slow and fast cases appear in the upper levels where the waves would be furthest from critical levels, and where vertical group velocities would be largest in theory [*Andrews et al.*, 1987].

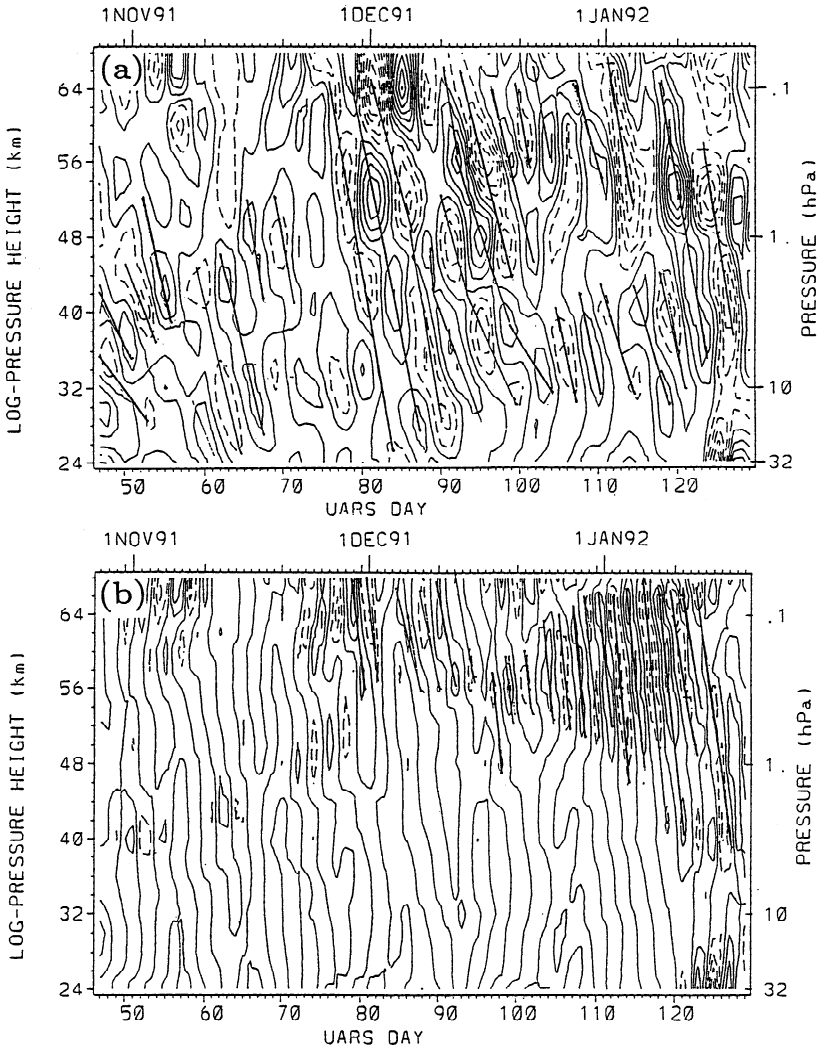

Figure 3. Height versus time diagram of zonal wave 1 for band-passed ISAMS equatorial temperatures at longitude 90°E. Half-amplitude filter response of (a) 4 to 16 days and (b) 3- to 5-day periods. Vertical scale: log-pressure heights (units kilometers) on left and pressure (units hectopascals) on right. Solid (dashed) contours begin at zero (-0.5) and increment (decrement) by 0.5. Units are Kelvin. Tilted line segments indicate downward phase propagation with time.

From Figure 3 it can be estimated that during the intense phase of the slower mode (days 76 through 106), the vertical wavelength of the perturbations is ~ 20 km. The 3 to 5-day feature has vertical wavelengths about twice as long.

Finally, Figure 4 shows that the features studied here exhibit equatorial trapping as predicted for Kelvin waves. Figure 4 shows time versus latitude plots of temperature, at 10 hPa (midstratosphere) and 1 hPa (near the stratopause). The amplitude peaks are centered on the equator and fall off appreciably for latitudes beyond about ±10°–15° latitude. This is consistent with Kelvin wave dynamics and with previous observational studies mentioned in the introduction. Figure 4 also indicates that there are times when the oscillations are not centered on the equator. These deviations are most likely due to the influence of latitudinal shear in the mean zonal flow [*Boyd*, 1982].

Comparison With MLS Data

The ISAMS temperature perturbations have been compared with traveling wave features identified in preliminary analyses of contemporaneous microwave limb sounder (MLS) temperature fields. Good agreement between the two data sets is found on Kelvin wave space-time scales (wave 1, 4 to 16-day periods). The comparison is made for the time period of UARS days 85–124 (December 5, 1991–January 13, 1992). A time series of the two data sets at 0° and 60°E longitude and 10 hPa and 1 hPa is shown in Figure 5. The two data sets with different measurement and gridding techniques deviate little at 10 hPa and only slightly more at 1 hPa on the fine scale of the Kelvin wave features presented in this paper.

Figure 6 shows a time series of the amplitude and phase of the wave 1 signal filtered for the band of fre-

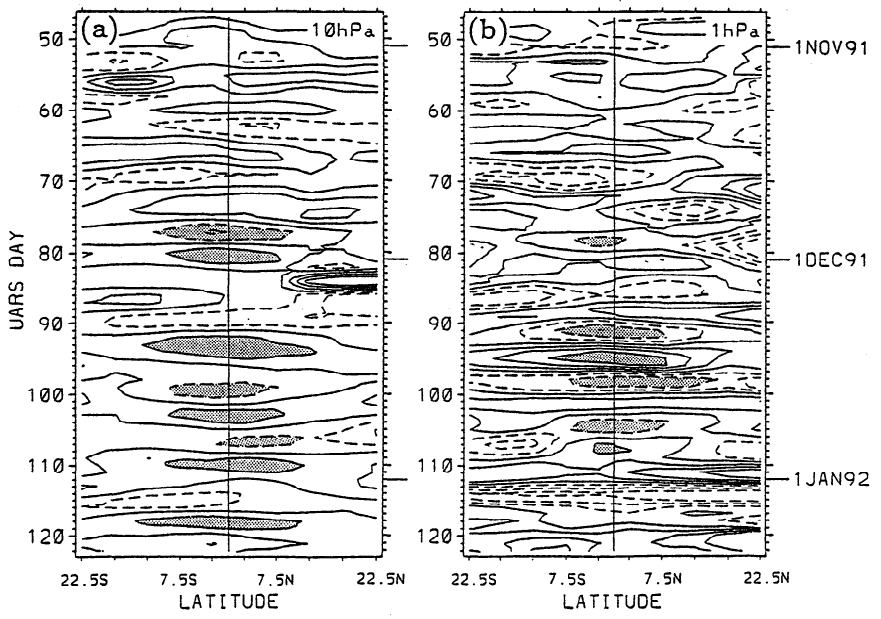

Figure 4. Time versus latitude diagrams of zonal wave 1 ISAMS band-passed (same as in Figure 2) temperatures at longitude 90°E and (a) 10 hPa and (b) 1 hPa pressure. Solid (dashed) contours start at zero (-0.5) and increment (decrement) by 0.5 K. Anomalies (positive or negative) confined within $\pm 10° - 15°$ latitude are shaded. Vertical line segment (center of each frame) indicates the equator.

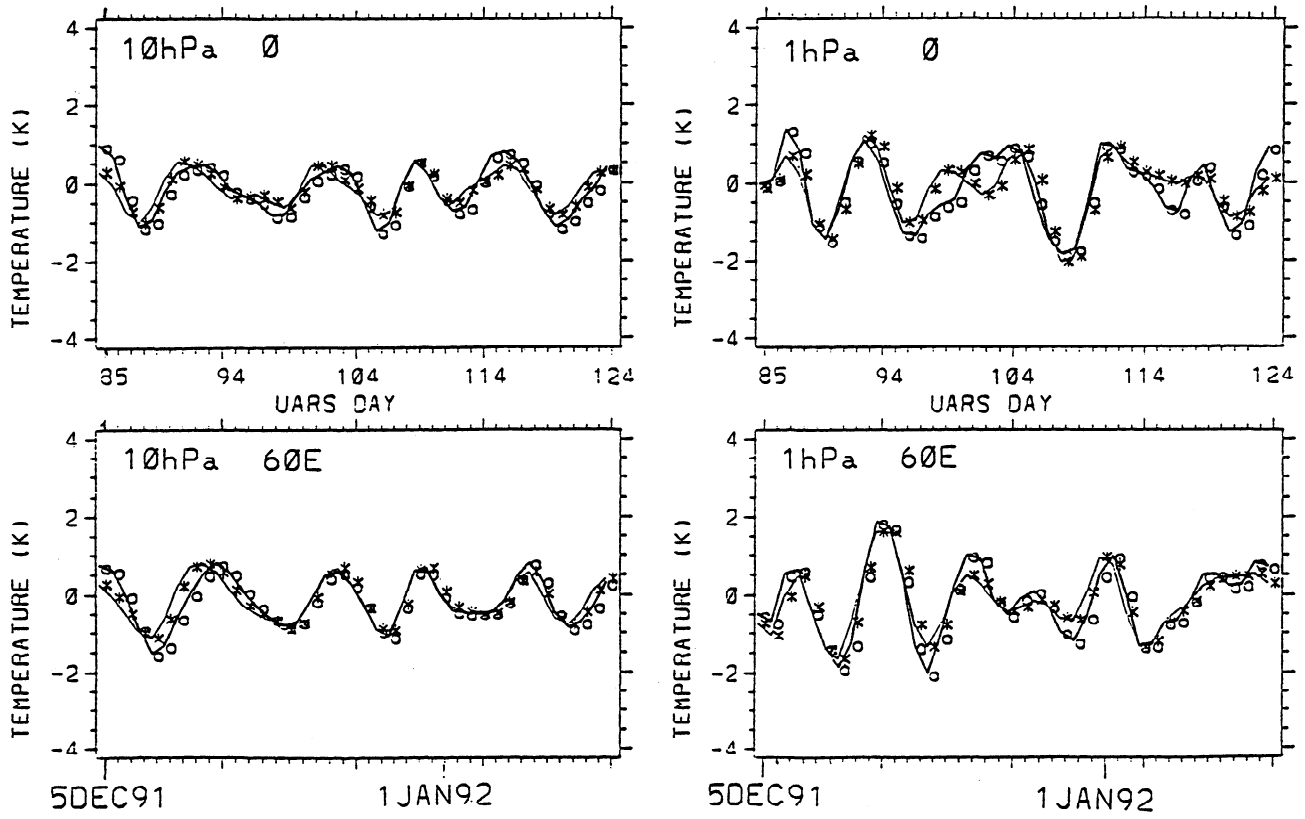

Figure 5. Temperature versus time diagrams of zonal wave 1 ISAMS and MLS band-passed filtered temperatures for 4- and 16-day half-amplitude response at 10 hPa and 1 hPa at the equator and 0° and 60°E longitude as indicated. ISAMS, asterisk; MLS, circle.

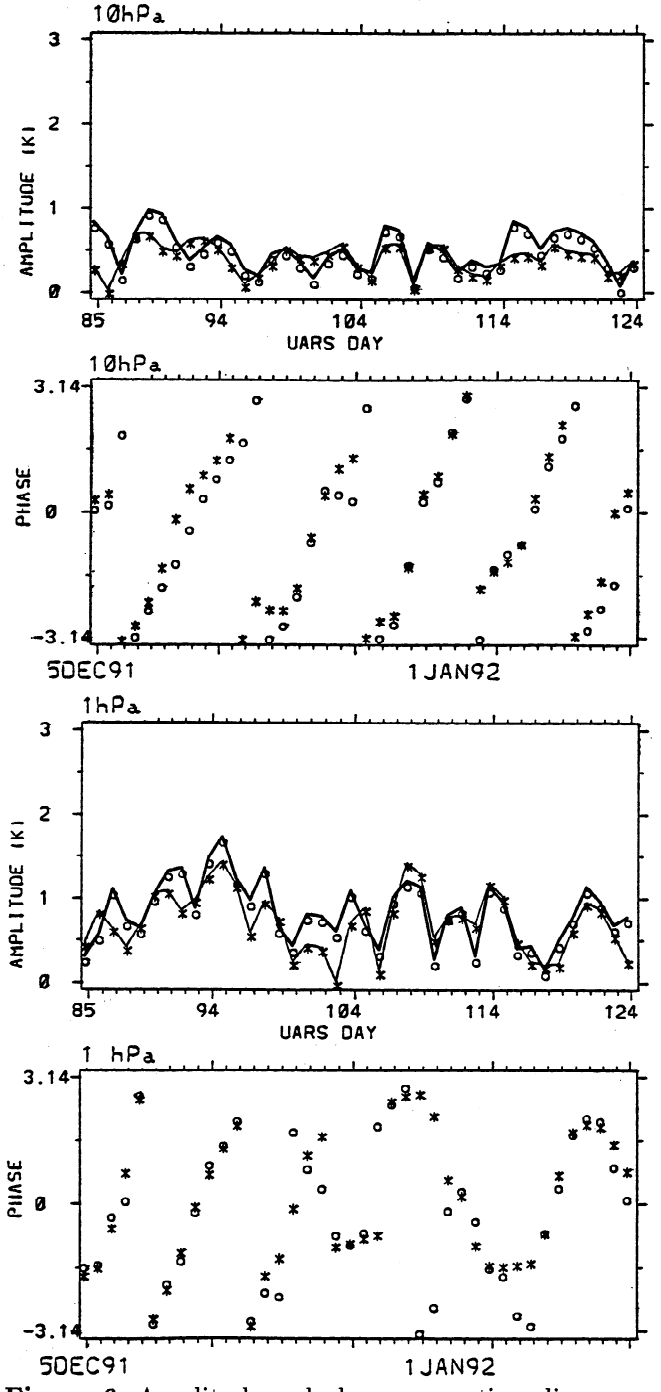

Figure 6. Amplitude and phase versus time diagrams of equatorial zonal wave 1 ISAMS and MLS band-passed filtered temperatures for 4- and 16-day half-amplitude response at 10 hPa and 1 hPa. ISAMS, asterisk; MLS, circle.

quencies of 4 to 16 days at 10 and 1 hPa. Again good agreement is seen, adding confidence to the existence of the Kelvin wave in this time period.

One noticeable difference seen in Figure 6 at 1 hPa is the zonal propagation after UARS day 108 (December 28, 1991). For days 109-111 MLS appears to show eastward propagation while ISAMS shows westward, though the phases are indeterminate by multiples of 2π, and this effect may not be real.

Canziani et al. [1994] also analyzed Kelvin waves in MLS data. At altitudes above 10 hPa, their Kelvin wave 1 phases do not agree with our results in Figures 5 and 6. Their approach, while making use of the coordinate rotation and FFT described above, differed in that they used latitude gridded (level 3AL) data which are unevenly spaced in time and longitude due to the variations in the orbital period described above. Because of this, and due to a programming error (P. O. Canziani, personal communication, 1994), differences between the two results might be expected.

Comparison of space-time spectral analysis on Kelvin wave scales is a rather sensitive and demanding test of both ISAMS and MLS instruments, their respective retrieval schemes and gridding procedures. We consider the agreement seen in Figures 5 and 6 to be very good. This suggests that both data sets are internally consistent at these spatial and temporal scales in the upper stratosphere and lower mesosphere.

5. Summary

The spectral decomposition and analyses presented in this paper reveal characteristics indicative of Kelvin wave behavior in upper stratospheric and lower mesospheric ISAMS temperature fields. These perturbations exhibit peak-to-peak amplitudes of 2–3 K, eastward phase progression, equatorial trapping, and episodic nature. The Kelvin wave periods decrease from $\sim$ 2 weeks at 10 hPa (32 km altitude) to about 1 week near 0.1 hPa (64 km altitude). Faster modes (3 to 5-day periods) are observed, but only in the lower mesosphere. The slower modes have vertical wavelengths $\sim$ 20 km while the faster 3 to 5-day mode has about twice this scale. Their downward phase progression and upward group velocity are consistent with upward propagation of energy from excitation at lower altitudes (presumably the troposphere). These characteristics are similar to those predicted by Kelvin wave dynamics and reminiscent of Kelvin waves found in earlier analyses of LIMS data at these altitudes.

Comparison with contemporaneous MLS temperature fields shows good agreement in details of Kelvin wave propagation characteristics. Because space-time spectral decomposition is sensitive to details of the retrieval and gridding processes, these results add credence to the integrity of both ISAMS and MLS data sets on spatial scales and timescales not possible to validate with zonal and time means. The agreement seen constitutes a rather demanding test of both ISAMS and MLS data sets and suggests good internal consistency at these spatial and temporal scales in the upper stratosphere and lower mesosphere.

Acknowledgments. The ISAMS data are the result of diligent work by the entire ISAMS team; the efforts of A. Dudhia and R. J. Wells are especially appreciated. We also

thank additional members of the MLS team for their valuable contributions in producing the MLS data. The ISU coauthors have been partially supported by National Aeronautics and Space Administration grants NAGW-2582 and NAG 5-2787. The Oxford coauthors have been sponsored by the U.K. Science and Engineering Research Council and the Natural Environment Research Council. Work at the Jet Propulsion Laboratory, California Institute of Technology, was performed under contract with the National Aeronautics and Space Administration.

References

Andrews, D. G., J. R. Holton, and C. B. Leovy, *Middle Atmosphere Dynamics*, 489 pp., Academic, San Diego, Calif., 1987.

Barath, F. T., et al., The upper atmosphere research satellite microwave limb sounder instrument, *J. Geophys. Res.*, *98*, 10,751-10,762, 1993.

Boyd, J. P., The influence of meridional shear on planetary waves, 2, Critical latitudes, *J. Atmos. Sci.*, *39*, 770-790, 1982.

Canziani, P. O., J. R. Holton, E. Fishbein, L. Froidevaux, and J. W. Waters, Equatorial Kelvin waves: A UARS-MLS view, *J. Atmos. Sci.*, *51*, 3053-3076, 1994.

Dudhia, A., and N. J. Livesey, Validation of Temperature Measurements from the Improved Stratospheric and Mesospheric Sounder, *J. Geophys. Res.*, in press, 1995.

Elson, L. S., and L. Froidevaux, The use of Fourier transforms for asynoptic mapping: Applications to the upper atmosphere research satellite microwave limb sounder, *J. Geophys. Res.*, *98*, 23039-23049, 1993.

Fishbein, E. F., et al., Validation of UARS MLS temperature/pressure measurements, *J. Geophys. Res.*, in press, 1995.

Hirota, I., Equatorial waves in the upper stratosphere and mesosphere in relation to the semiannual oscillation of the zonal wind, *J. Atmos. Sci.*, *35*, 714–722, 1978.

Hirota, I., M. Shiotani, T. Sakuri, and J. Gille, Kelvin waves near the equatorial stratopause as seen in SBUV ozone data, *J. Meteorol. Soc. Jpn.*, *69*, 179-186, 1991.

Lait, L. R., and J. L. Stanford, Applications of asynoptic space-time Fourier transform methods to scanning satellite measurements, *J. Atmos., Sci.*, *45*, 3784-3799, 1988.

Murakami, M., Large-scale aspects of deep convective activity over the GATE area, *Mon. Weather. Rev.*, *107*, 994–1013, 1979.

Prata, A. J., Traveling waves in Nimbus-7 SBUV ozone measurements: Observations and theory, *Q. J. R. Meteorol. Soc.*, *116*, 1091–1122, 1990.

Randel, W. J., Kelvin wave-induced trace constituent oscillations in the equatorial stratosphere, *J. Geophys. Res.*, *95*, 18,641–18,652, 1990.

Randel, W. J., and J. C. Gille, Kelvin wave variability in the upper stratosphere observed in SBUV ozone data, *J. Atmos. Sci.*, *48*, 2336–2349, 1991.

Rodgers, C. D., et al., *Improved stratospheric and mesospheric sounder version 8 validation report, ISAMS Doc. SW340*, p. 114, Univ. of Oxford, Oxford, England, 1994.

Salby, M. L., Sampling theory for asynoptic satellite observations, I, Space-time spectra, resolution, and aliasing, *J. Atmos. Sci.*, *39*, 2577-2600, 1982a.

Salby, M. L., Sampling theory for asynoptic satellite observations, II, Fast Fourier synoptic mapping, *J. Atmos. Sci.*, *39*, 2601-2614, 1982b.

Salby, M. L., D. L. Hartmann, P. L. Bailey, and J. C. Gille, Evidence for equatorial Kelvin modes in Nimbus-7 LIMS, *J. Atmos. Sci.*, *41*, 220–235, 1984.

Salby, M. L., P. Callaghan, S. Solomon, and R. R. Garcia, Chemical fluctuations associated with vertically propagating equatorial Kelvin waves, *J. Geophys. Res.*, *95*, 20,491–20,505, 1990.

Taylor, F. W., Pressure modulator radiometry, in *Spectrometric Techniques*, vol. 3, pp. 137-197, Academic, San Diego, CA, 1983.

Taylor, F. W., et al., Remote sensing of atmospheric structure and composition by pressure modulator radiometry from space: The ISAMS experiment on UARS, *J. Geophys. Res.*, *98*, 10,799–10,814, 1993.

Ziemke, J. R., and J. L. Stanford, One-to-two month oscillations in the stratosphere during southern winter, *J. Atmos. Sci.*, *47*, 1778–1793, 1990.

Ziemke, J. R., and J. L. Stanford, Kelvin waves in total column ozone, *Geophys. Res. Lett.*, *21*, 105–108, 1994.

D. R. Allen, J. L. Stanford, E. M. Stone, and J. R. Ziemke, Department of Physics and Astronomy, Iowa State University, Ames, IA 50011.

L. S. Elson, E. F. Fishbein, and J. W. Waters, Jet Propulsion Laboratory, California Institute of Technology, Pasadena, CA.

B. N. Lawrence, C. D. Rodgers, and F. W. Taylor, Department of Atmospheric, Oceanic and Planetary Physics, University of Oxford, Oxford, England.

(Received August 22, 1994; revised December 19, 1994; accepted March 18, 1995.)